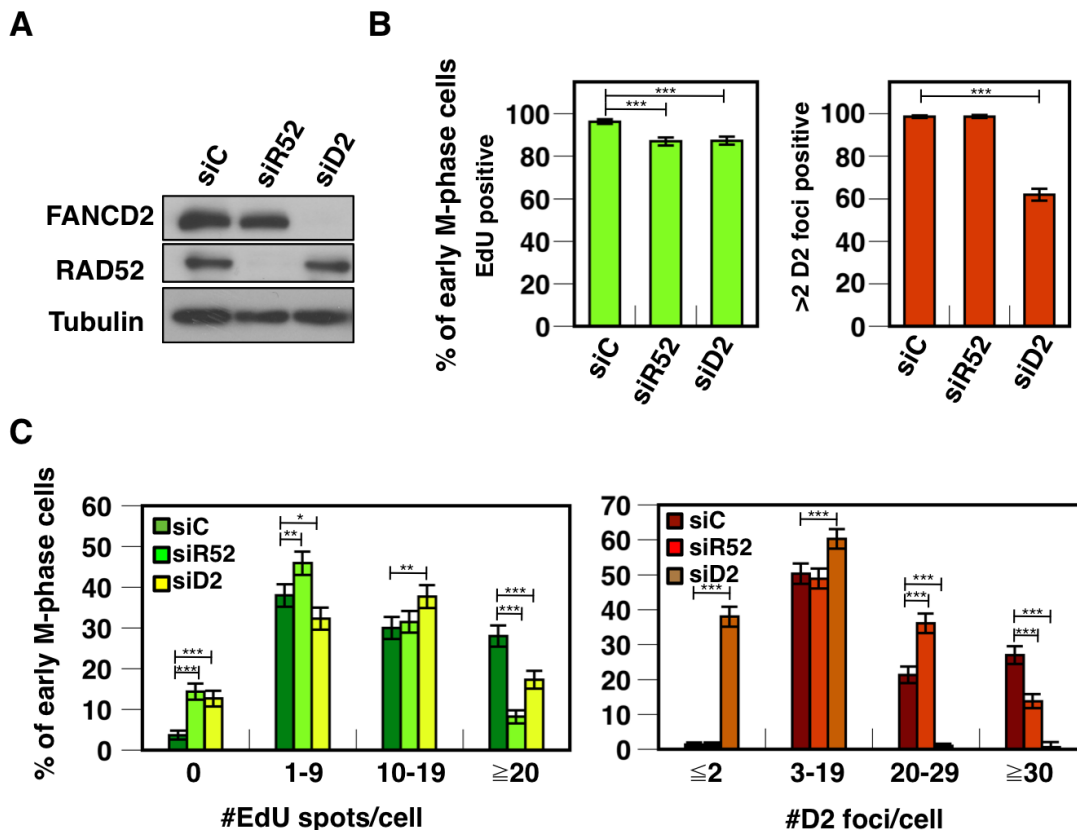


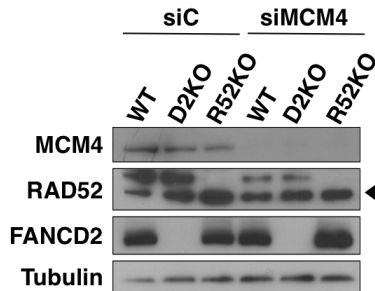
HCT116



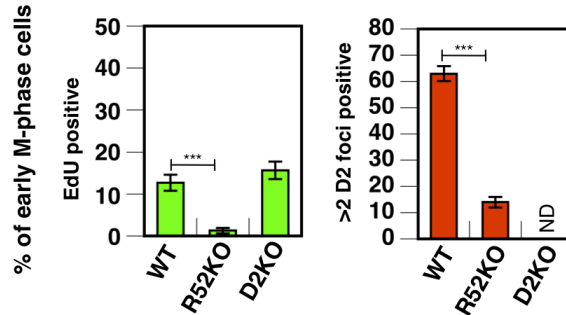
Supplementary Figure 1. Depletion of RAD52 or FANCD2 in WT HCT116 cells phenocopies R52KO or D2KO cells, respectively. **A.** Immunoblotting to show depletion of RAD52 or FANCD2 in wild-type cells along with siC-treated sample. Tubulin was used as a loading control. **B.** Percentage of early M-phase (prophase to pro-metaphase) cells positive for EdU spots (left) or >2 FANCD2 foci (right) per siRNA treatment group after Aph treatment. **C.** Distribution of cells harboring respective ranges of EdU spots (left) or FANCD2 foci (right) per siRNA treatment group. Depletion of RAD52 or FANCD2 also decreased the fraction of cells with ≥ 20 EdU spots. Unlike R52KO cells, WT cells depleted for RAD52 did not show a decrease in the overall percentage of cells positive for >2 FANCD2 foci, but they displayed a significantly lower number of cells containing >30 FANCD2 foci (right). Error bars indicate standard deviations of respective frequencies. *, ** and *** indicate $p < 0.05$, $p < 0.01$ and $p < 0.001$ by a χ^2 -test.

HCT116

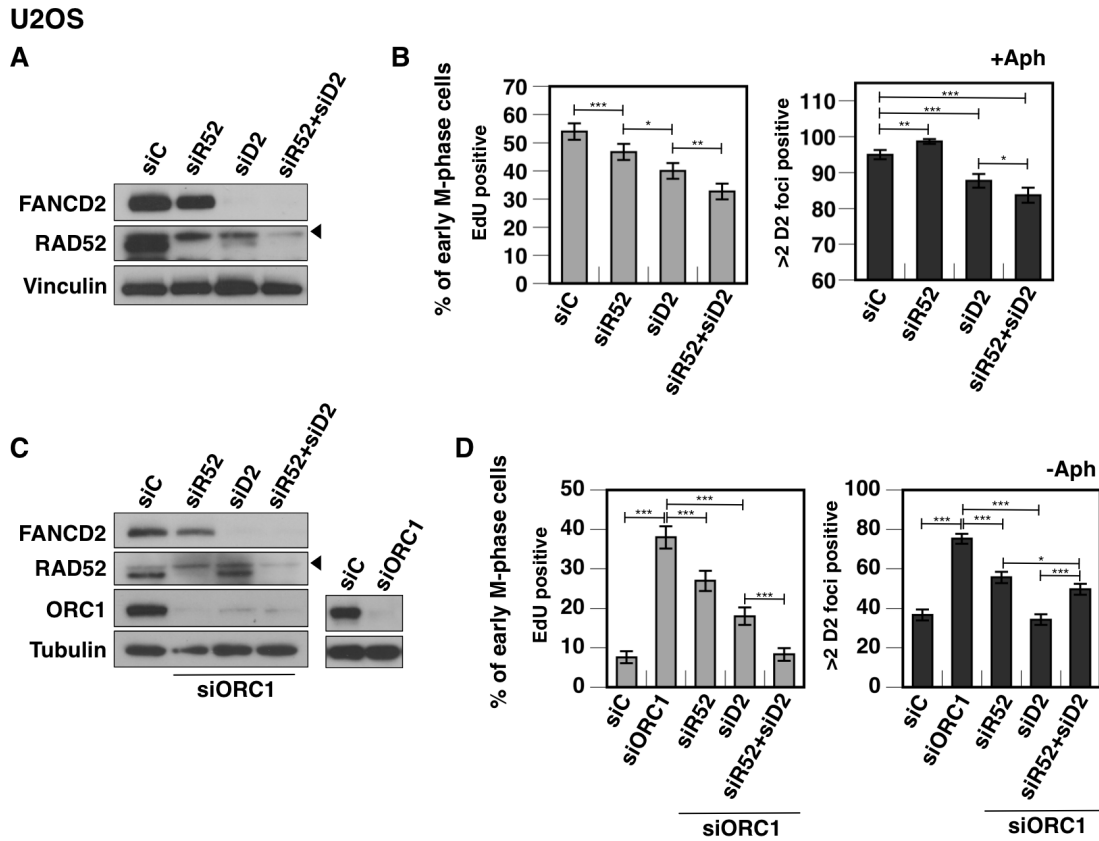
A



B

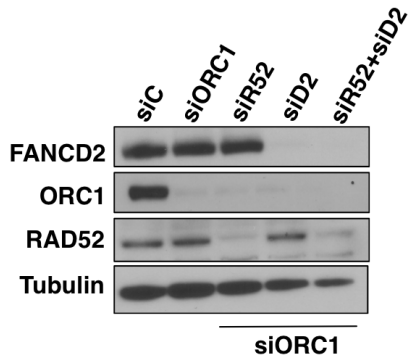


Supplementary Figure 2. Depletion of MCM4 is relatively inefficient in inducing EdU spot formation in HCT116 cells. **A.** Immunoblotting to show depletion of MCM4 in respective genotypes. Tubulin was used as a loading control. A triangle indicates a non-specific band detected by the RAD52 antibody. **B.** Percentage of early M-phase cells positive for EdU spots (left) or >2 FANCD2 foci (right) after MCM4 depletion. Error bars indicate standard deviations of respective frequencies. *** indicates $p < 0.001$ by a χ^2 test. ND: None detected. siMCM4 (D-003275-05) was purchased from Dharmacon. Anti MCM4 antibody (ab4459) was used at 1:7000.

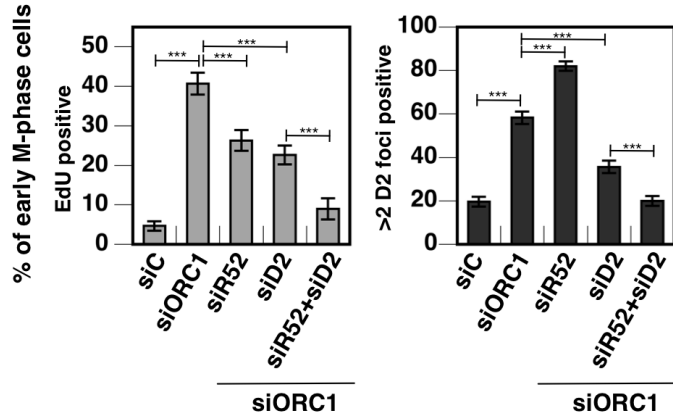


Supplementary Figure 3. The formation of Aph- or siORC1- induced EdU spots depends both on RAD52 and FANCD2 in U2OS cells. **A.** Immunoblotting to show depletion of RAD52 and/or FANCD2. Vinculin was used as a loading control. **B.** Percentage of early M-phase cells positive for EdU spots (left) or >2 FANCD2 foci (right) per siRNA treatment group after APH treatment. **C.** Immunoblotting to show RAD52 and/or FANCD2 with ORC1 depletion (left) or single depletion of ORC1 (right). **D.** Percentage of early M-phase cells positive for EdU spots (left) or >2 FANCD2 foci (right) after ORC1 depletion in combination with RAD52 and/or FANCD2 depletion. In **A** and **C**, filled triangles indicate a non-specific band detected by the RAD52 antibody. In **B** and **D**, error bars indicate standard deviations of respective frequencies. *, **, and *** indicate $p < 0.05$, $p < 0.01$ and $p < 0.001$ by a χ^2 - test, respectively. While depletion of RAD52 consistently impaired EdU spot formation, its effect on FANCD2 foci was inconsistent. It either increased (siR52 in **B**, siR52+siD2 in **D**) or decreased (siR52+siD2 in **B**, siR52 in **D**) FANCD2 foci.

HeLa
A

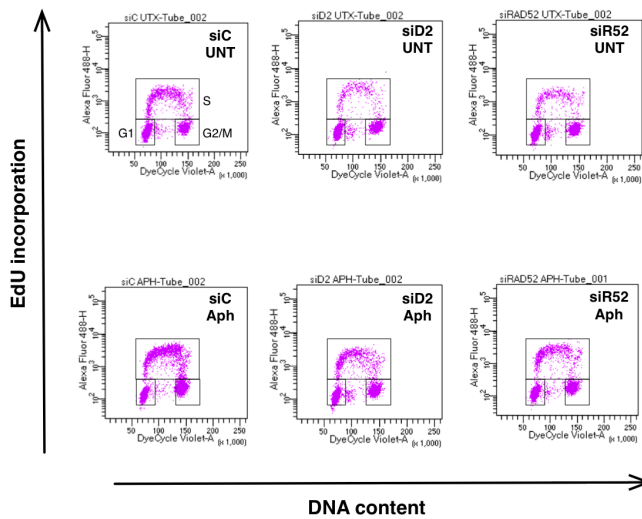


B

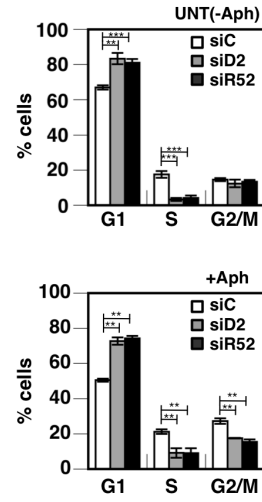


Supplementary Figure 4. The formation of EdU spots depends both on RAD52 and FANCD2 in HeLa cells. **A.** Immunoblotting to show RAD52 and/or FANCD2 with ORC1 depletion or single depletion of ORC1 in HeLa cells. Tubulin was used as a loading control. **B.** Percentage of early M-phase cells positive for EdU spots (left) or >2 FANCD2 foci (right). In **B**, error bars indicate standard deviations of respective frequencies. *** indicates $p < 0.001$ by a χ^2 -test. Like U2OS cells, depletion of RAD52 consistently impaired EdU spot formation. However, its effect on FANCD2 foci was inconsistent. Single depletion of RAD52 increased the number of cells with FANCD2 foci, but its co-depletion with FANCD2 further impaired FANCD2 focus formation relative to FANCD2 single depletion.

RPE1
A



B

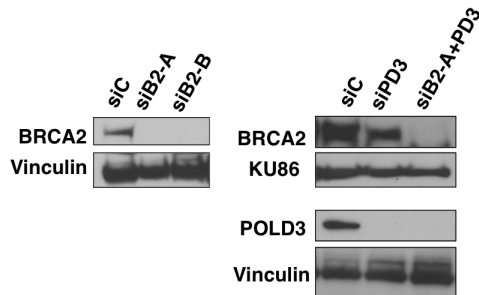


Supplementary Figure 5. Depletion of FANCD2 or RAD52 confers similar cell cycle profiles.

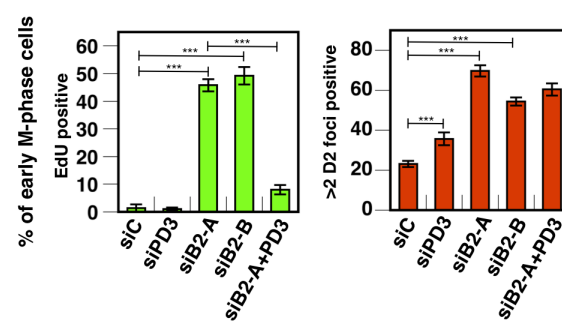
A. Representative images of two-color plots by flow cytometry. After 48 hrs of incubation with siRNA, cells were harvested for a cytometric assay, which was performed using Click-iT™ Plus EdU Alexa Fluor™ 488 Flow Cytometry Assay Kit and FxCycle™ Violet Stain (Invitrogen, C10632, F10347, respectively). Small squares in each plot represent cells in the S, G1, and G2/M phases, respectively. **B.** Percentage of cells in the G1, S, and G2/M phases in the absence of Aph treatment (top), or after Aph treatment for 24 hrs (bottom). Relative to siC-treated conditions, depletion of FANCD2 or RAD52 caused a sharp decline in S-phase cells and an increase in G1-phase cells in the presence/absence of Aph treatment. Overall, Aph treatment caused the accumulation of cells in the S and G2/M phases. Error bars indicate standard errors of the mean. ** and *** indicate $p < 0.001$ and $p < 0.0001$ by a t-test, respectively.

RPE1

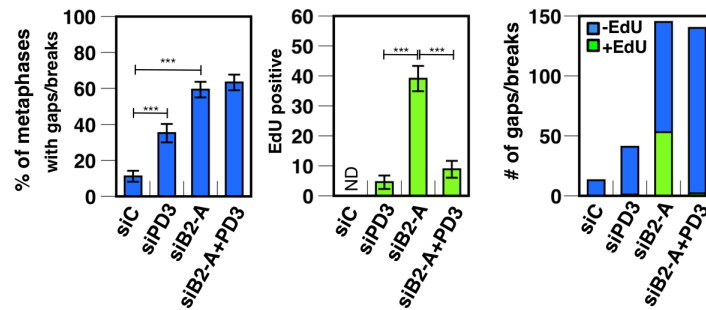
A



B



C



Supplementary Figure 6. EdU spots induced by BRCA2 depletion display the characteristics of mitotic DNA synthesis. **A.** Immunoblotting to show depletion of BRCA2 (left) or POLD3 (right) and co-depletion of BRCA2 and POLD3 (right). Vinculin or KU86 was used as a loading control, respectively. **B.** Percentage of early M-phase cells positive for EdU spots (left) or >2 FANCD2 foci (right) per siRNA treatment group. **C.** Percentage of metaphase cells with gaps/breaks (left) and of those with EdU spots (middle), and the total number of gaps/breaks detected in 120 cells scored (right) per siRNA treatment. The percentage of cells with chromosome aberrations did not decrease in cells depleted for BRCA2 and POLD3, but nearly all gaps/breaks occurred in the absence of EdU spots. Error bars indicate standard deviations of respective frequencies in **B** and **C**. *** indicates $p < 0.001$ by a χ^2 -test in **B** and **C**. ND: None detected. siBRCA2-A and -B (BRCA2HSS101095, BRCA2HSS101097) were purchased from Thermo Fisher. Anti-BRCA2 (Sigma OP-95, 1:500) antibody was used for immunoblots.

Supplementary Methods: Generation of RAD52 deficient lines in RPE1 cells by CRISPR/Cas9 editing

A sense-stranded guide RNA targeting exon 3 of RAD52 (5'-UACAUAAAGUAGCCGCAUGGC-3') was purchased from Synthego as a 100 nucleotide sgRNA. One hundred pmol Synthego RAD52 exon 3 sgRNA was electroporated into RPE1 cells along with 1 ug CleanCap 3XNLS Cas9 mRNA (TriLink) using a Neon electroporator (Invitrogen). Two days later, cells were trypsinized and plated in wells of 96-well plates (1-3 cells per well). Cells were allowed to expand and were transferred to duplicates of 48-well plates; one for preparing frozen stocks of individual populations and the other for genomic DNA isolation. To confirm CRISPR/Cas9 editing of RAD52 exon 3, PCR was performed using a primer pair that spans exon 3 of RAD52 (ScrF 5'-TGTGAGGAATGGTGGAAAGTGT-3' and ScrR 5'-TTAAGACGGCGGTTATGCGA-3') to produce a 366 bp amplicon. Resulting amplicons were Sanger sequenced to identify clonal populations with bi-allelic editing including clones B7 and D8, which were used in this study. As shown below, these clones have frameshift mutations at both alleles (highlighted in yellow). In the following sequence of RAD52 exon3, the sgRNA sequence is underlined.

Clone B7

#1 A 23 bp deletion

TGC CAG TAC ACA GCA GAA GAG TAC CAG GCC ATC CAG AAG GCC CTG AGG CAG AGG
CTG GGC CCA GAA TA**(-C ATA AGT AGC CGC ATG GCT GGC GGA GGC CAG A)**AG

#2 An insertion of T

TGC CAG TAC ACA GCA GAA GAG TAC CAG GCC ATC CAG AAG GCC CTG AGG CAG AGG
CTG GGC CCA GAA TAC ATA AGT AGC CGC AT**(+T)**GGC TGG CGG AGG CCA GAA G

Clone D8

#1 A 17 bp deletion

TGC CAG TAC ACA GCA GAA GAG TAC CAG GCC ATC CAG AAG GCC CTG AGG CAG AGG
CTG GGC CCA GAA TAC ATA AGT**(-AGC CGC ATG GCT GGC GG)**A GGC CAG A)AG

#2 An insertion of T

TGC CAG TAC ACA GCA GAA GAG TAC CAG GCC ATC CAG AAG GCC CTG AGG CAG AGG
CTG GGC CCA GAA TAC ATA AGT AGC CGC AT**(+T)**GGC TGG CGG AGG CCA GAA G

The above procedures were performed at the University of Minnesota/Masonic Cancer Center Shared Resource: Genome Engineering Shared Resource (GESR).